Available online at www.sciencedirect.com

ScienceDirect

Geochimica et Cosmochimica Acta 75 (2011) 4125–4139

Geochimica et Cosmochimica Acta

www.elsevier.com/locate/gca

Glass–water interphase reactivity with calcium rich solutions

T. Chave [a,b,*], P. Frugier [a], S. Gin [a], A. Ayral [c]

[a] CEA Marcoule, DTCD/SECM/LCLT, BP 17171, 30207 Bagnols-sur-Cèze Cedex, France
[b] ICSM – UMR 5257 CEA-CNRS-UMII-ENSCM, BP 17171, 30207 Bagnols-sur-Cèze Cedex, France
[c] IEM/CNRS-ENSCM-UM2 Université de Montpellier 2, CC 047, Place Eugène Bataillon, 34095 Montpellier Cedex 5, France

Received 24 March 2010; accepted in revised form 24 March 2011; available online 10 May 2011

Abstract

The effect of calcium on synthetic glass alteration mechanisms has been studied. It is known that the higher the calcium content in the glass, the higher the forward rate. However, in a confined medium reaching apparent saturation state and a $pH_{90°C}$ around 9, synthetic calcium-bearing glasses are those with the lowest alteration rates. This work brings new and fundamental evidence toward understanding the alteration mechanisms: the rate-decreasing effect of calcium exists even if the calcium comes from the solution. Calcium from solution reacts with silica network in the hydrated layer at the glass surface. The calcium effect on the alteration kinetics is explained by the condensation of a passivating reactive interphase (PRI) whose passivating properties are strongly enhanced when calcium participates in its construction. These experiments provide new evidence of the role of condensation mechanisms in glass alteration. This better understanding of the calcium effect on glass long-term behavior will be useful both for improving glass formulations and for understanding the influence of the water composition.

1. INTRODUCTION

Many fields of research are concerned by water–rock interactions ranging from global cycling of elements to the transport of groundwater nutrients and contaminants. Mineral surface descriptions are required to understand the mechanisms involved. Many multi-oxide mineral surfaces exposed to aqueous solution exhibit metal-depleted proton-enriched compositions. The depth to which cations are leached from the surface depends on various parameters: mineral composition, pH, time, temperature, solution saturation state and even the ion concentrations in solution (Muir and Nesbitt, 1997). A large number of multi-oxide minerals are concerned by this mechanism, including labradorite feldspar (Chardon et al., 2006), albite (Hellmann, 1997), wollastonite (Schott et al., 2002; Daval et al., 2009), and forsterite (Pokrovsky and Schott, 2000). For Oelkers et al. (2009), the metal–proton exchange reactions could play a major role in controlling the alteration kinetics of many multi-oxide silicate minerals, including glasses.

The removal of mono- and divalent cations from a mineral creates new "internal" surface sites accounting for proton consumption from solution (Oelkers et al., 2009). The number of protons consumed could even depend on the repolymerization of the mineral surface during leaching (Casey et al., 1993). Theoretical considerations based on Monte Carlo simulations led to assert that an interfacial dissolution–reprecipitation mechanism dominates feldspar dissolution (Zhang and Lüttge, 2009). The role of condensation mechanisms on mineral dissolution kinetics is obviously an issue raised by more and more authors (Casey et al., 1993; Oelkers et al., 2009; Zhang and Lüttge, 2009).

In the field of glass alteration, condensation mechanisms forming amorphous layers have also long been a subject of interesting debates. Many glass dissolution studies focus on mechanisms responsible for the alteration rate drop when the solution becomes enriched in elements arising from dissolution. The rate drop is mainly understood as the onset of

* Corresponding author at: Laboratoire de Sonochimie dans les Fluides Complexes, Institut de Chimie Séparative de Marcoule, UMR 5257 – ICSM Site de Marcoule, BP 17171, 30207 Bagnols-sur-Cèze Cedex, France. Tel.: +33 (0)4 66 33 92 50.
E-mail address: tony.chave@cea.fr (T. Chave).

0016-7037/$ - see front matter © 2011 Elsevier Ltd. All rights reserved.
doi:10.1016/j.gca.2011.05.005

a saturation state. Historically, this apparent saturation state was expressed in equations as if an equilibrium with the fresh glass could be achieved (Advocat et al., 1995). Today authors consider that a saturation state can only be written with respect to a hydrated layer that passivates the underlying fresh glass (Bourcier et al., 1990; Gin and Jegou, 2002; Cailleteau et al., 2008). This passivation is rarely fully effective and consequently transport by diffusion must be added to classical affinity laws to fully model glass alteration. Interdiffusion refers to the reactive transport of water from solution to the fresh glass, and solvated ions (alkali metals, boron, etc.) from the fresh glass into solution through the passivating hydrated layer. Interdiffusion coefficients are consistent with diffusion in solids with values of the order of magnitude of 10^{-20} m^2 s^{-1}. Moreover, the activation energy of interdiffusion coefficients is higher than that for ionic diffusion in water (Chave et al., 2007). This high value is consistent with the breaking of bonds controlling the overall process. For several authors, the resulting reactive transport applies mainly to fresh glass (Grambow and Muller, 2001) or mainly to a surface layer, reactive with regard to the solution, and constituting the locus of ongoing dissolution and condensation phenomena (Frugier et al., 2008). Frugier et al. (2008) denominated “Passivating Reactive Interphase” (PRI) the transitional zone in which chemical gradients of alkali metals and boron develop. In the present paper two denominations will be used:

- Hydrated surface layer (Bunker et al., 1988) will be used as a general vocabulary not implying any specific properties like potential passivation of underlying glass or formation mechanism as a residual glass structure, by local condensation mechanisms or full dissolution/precipitation process.
- Passivating reactive interphase will be used to designate the hydrated surface layer, or the part of it, that limits interdiffusion process. Such vocabulary is useful for making the difference between obvious experimental results such as “an hydrated surface layer is formed” and hypothetical properties under discussion within the framework of a model such as “the interdiffusion coefficient within the PRI is temperature dependent”.

The presence of a hydrated surface layer raises two questions: is it able to control the saturation state in solution of the elements it contains, and does it control interdiffusion by limiting water access to the glass? This paper focuses on interdiffusion kinetic, please refer to (Rajmohan et al., 2010) regarding saturation state control of the solution.

In order to better understand the role played by this layer, the effect of a cation not belonging to the glass but available in solution has been studied. Classical glass alteration laws use an affinity function which does not take into account elements that do not belong to the glass (Daux et al., 1997). Moreover, many authors consider interdiffusion as a process taking place within the glass structure and relatively independent of solution chemistry (Grambow and Muller, 2001). Consequently an element not belonging to the glass should have no major effect on the alteration kinetics. Demonstrating the contrary would provide an opportunity to confirm the major role of condensation mechanisms within this hydrated layer on the dissolution and interdiffusion mechanisms.

Calcium was selected for this study. Calcium belonging to the glass was shown by Jegou et al. (1999) to strongly enhance the alteration rate drop in a closed system. Our goal is to determine whether this effect of calcium on the glass alteration kinetics comes mainly from its effect on the glass structure or from its availability in solution. We believe that answering this question can contribute to understanding the role of condensation mechanisms on the alteration kinetics of glass, and potentially of multi-oxide silicates.

2. STATE OF THE ART

Bunker et al. early described the possible simultaneous reactions occurring between glass and aqueous solution including (i) hydration, in which water enters the glass as solvent, (ii) hydrolysis/condensation, in which water reacts with metal–oxygen bonds to form hydroxyl groups and (iii) ion exchange reactions, in which modifier cations such as sodium are replaced by protons or other cations (Bunker et al., 1988; Bunker, 1994).

Recent published studies relative to glass alteration generally approach the process by a phenomenological description involving five rate regimes (Van Iseghem et al., 2007):

(1) Initial interdiffusion
(2) The initial or forward rate
(3) The rate drop
(4) The residual rate
(5) A possible resumption of alteration in particular conditions

This approach based on the observation of alteration kinetics, which in turn are determined from concentration variations of the mobile elements (boron, alkali metals) in solution, can be related to the nature of the underlying mechanisms. The correlations between the kinetic regimes and these mechanisms are not trivial and are sometimes subject to different interpretations. Two recent reviews of these mechanisms are available (Conradt, 2008; Frugier et al., 2008). This second paper gives details about two major issues in the literature: the affinity function and interdiffusion (Frugier et al., 2008).

2.1. Affinity function

Most authors use affinity functions to model glass alteration kinetics, although there is no agreement about the precise nature of the phase toward which the equation should be written. The consequence is a poor agreement on the elements that must be taken into account in the affinity term. Early models (Advocat et al., 1995) applied the affinity function to the whole glass composition. However, it is clear that thermodynamic equilibrium between the glass and solution is challenged by a simple observation: it is impossible to create an alkali-bearing glass from an aqueous solution. Concepts have changed and the affinity function is now written with respect to a hydrated layer formed at the glass/water interface. Some authors call it "hydrated glass" (Grambow and Muller, 2001), others call it a "gel" (Spalla et al., 2004) depending on whether they consider it mainly as a residual solid (hydrated glass) or a reorganized solid (gel). Nevertheless, both mechanisms should account for the structure of this layer. Frugier et al. (2008) call it "passivating reactive interphase" (PRI) based more on its properties than on its structure. For Oelkers (2001) and Oelkers et al. (2009) thermodynamic equilibrium should no longer be written with respect to fresh glass once a hydrated layer is produced by an ion exchange reaction: the activated complex (still assumed by many authors to control the overall glass reaction) should contain elements in agreement with the composition of the hydrated layer. Applying the activated complex theory to basaltic glass, Daux et al. (1997) used the hydrated layer's stoichiometry for the affinity functions. Ultimately the same elements can be taken into account in the affinity function describing glass dissolution, leading to the same mathematics formalism for the glass dissolution law whatever the underlying theory, activated complex or chemical affinity with respect to a passivating layer. However, considering a chemical affinity with respect to a passivation layer, this solid phase must be taken into account in the mass balance of the reaction.

2.2. Interdiffusion

The term interdiffusion, as reported in the literature, refers to the exchange between glass network-modifying cations and protons in solution. This mechanism has been identified experimentally during the leaching of many minerals and natural glasses, especially in acidic media (Doremus, 1975). The interpretation is based on the observation of inversely correlated sigmoidal concentration profiles in the hydrated glass between alkali ions and protons. Its diffusive nature makes this the overriding phenomenon during the initial moments of glass or mineral leaching. Some questions remain regarding the detailed atomic-scale mechanism leading to this macroscopic phenomenon. The first concerns the elements involved and the nature of the material in which diffusion occurs. For some authors (Grambow and Muller, 2001; Verney-Carron et al., 2007) the process mainly concerns the glass structure and alkali metals not involved in the glass-forming network. For others (Spalla et al., 2004; Frugier et al., 2008; Jollivet et al., 2008; Zhang and Lüttge, 2008) the passivating properties of the condensed hydrated layer can forbid water penetration; this explains why other elements, like boron, can exhibit the same behavior than alkali metals although their structural role in the glass is completely different from that of alkali metals (Ferrand et al., 2006; Geneste et al., 2006; Ojovan et al., 2006; Chave et al., 2007).

Debates around these mechanisms are based mainly on experiments performed in initially pure water. Leach tests in initially pure water are usually the first logical step when studying glass alteration. Nevertheless, as pointed out by (Lüttge, 2006) they are not sufficient to understand the limits of such models and theories. The current study follows that path.

In 1998, several CEA studies sought to understand the behavior and importance of the major glass matrix components. Gin and Jegou (2001) studied simplified glasses with the stoichiometry of French reference nuclear glass (glass compositions are given in Table 1). Leach tests were performed in closed systems at 90 °C for a solution to volume (S/V) ratio of 80 cm^{-1}. At such a high S/V ratio, apparent equilibrium conditions for silicon in solution were reached in a few days. Nevertheless, this did not prevent the boron and alkali concentrations from rising in solution. In Fig. 1, it can be seen that Ca causes a strong kinetic drop especially when combined with both Al and Zr as a glass component. However, we can wonder whether the calcium effect still exists when it is not available in the glass but comes from solution. Calcium provided from solution has never been proved to decrease alteration rate. However, according to Berger et al. (1987), magnesium coming from seawater can decrease interdiffusion kinetic within basaltic glass alteration layer at 200 and 320 °C, even if it mainly precipitates as smectites on the external surface of the amorphous layer.

3. MATERIALS AND METHODS

3.1. Experimental approach

In order to study the effect of calcium when it is only available in solution, it is of course necessary to choose a simple glass without calcium. The five-oxide glass containing Si, B, Na, Al and Zr appears to be a good choice:

- It does not contain elements that drive smectite precipitation, such as Ni or Zn. A fully amorphous alteration layer will simplify both characterization and modeling.
- It contains Al and Zr which both decrease Si activity in solution and prevent the formation of hydrated calcium silicate (Rajmohan et al., 2010).

Table 1
Composition of the simplified glass and the French reference nuclear glass (FRNG) expressed in oxide weight percent.

	SiO_2	B_2O_3	Al_2O_3	Na_2O	Li_2O	Cs_2O	CaO	Fe_2O_3	ZrO_2	ZnO	Nd_2O_3	La_2O_3	Pr_2O_3	Ce_2O_3	Others
FRNG	45.5	14.0	4.9	9.9	2.0	1.1	4.0	2.9	2.7	2.5	1.6	0.9	0.5	1.0	6.5
Si B Na	65.6	20.2		14.2											
Si B Na Al	61.2	18.9	6.6	13.3											
Si B Na Al Ca	58.1	17.9	6.3	12.6			5.1								
Si B Na Al Ca Zr	56.2	17.3	6.1	12.2			5.0		3.2						
Si B Na Al Zr	59.1	18.2	6.4	12.8					3.5						

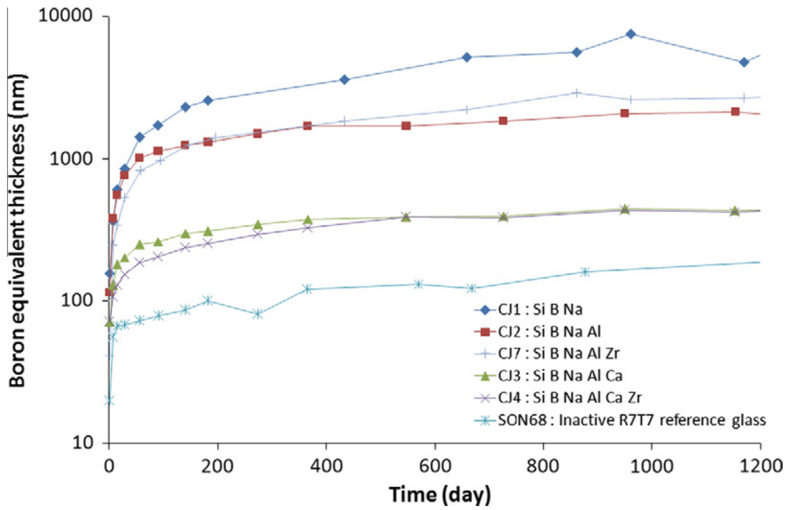

Fig. 1. Glass composition effect on the kinetic drop for different simple glass compositions with the stoichiometry of the R7T7 reference glass (Jegou, 1998) at 90 °C and 80 cm^{-1}. Apparent saturation with respect to silica is reached in a few days due to the high S/V ratio. The main process driving dissolution over the 3 years is reactive diffusion. pH values are around 9.0 (at 90 °C) and relatively independent of the glass composition and time.

- It contains the main French reference nuclear glass elements. As observed in Fig. 1, the Si–B–Na–Al–Zr-Ca simple glass dissolution kinetic is comparable to those of the French reference nuclear glass.

The chosen glass composition is given in Table 1.

The test glass was melted at 1400 °C in a platinum crucible in an induction-heated melter as described in Gin and Jegou (2001). The homogeneity of glass melts with similar compositions has already been verified by Rayleigh–Brillouin scattering; the Landau–Placzek ratios ranged from 50 to 200, indicating that these glasses contained no heterogeneities exceeding 15 Å (Jegou et al., 1999). In view of its composition our simplified glass was also assumed to be homogeneous. The glass samples were ground and sieved to recover the 40–100 µm fraction. The powders were cleaned several times in acetone by sedimentation to remove all the fine particles remaining on the glass surface. Four different powder batches from a single glass batch, but separately ball-milled and washed, were used in this study. All samples were characterized by krypton BET measurement with a Micrometrics ASAP 2010 analyzer. Data concerning these materials are given in Table 2.

Slow kinetics are expected after the rate drop. All the experiments were therefore carried out at a high surface-to-solution–volume ratio and at 90 °C to allow precise measurement of the leach rates, and with a pH of 8.7 (measured at 90 °C).

The experiments are divided in two sets: the first was intended to investigate the effect of the calcium concentration (experiments I–VII) and of prior glass alteration (experiments VIII–X), The second set (experiments XI–XIV) was specifically designed for characterization of the leached layer by Time-Of-Flight Secondary Ion Mass Spectrometry (TOF-SIMS) as explained later. The experimental conditions are indicated in Tables 3 and 4, respectively.

The references "A" and "B" are used to designate experiments where solution renewal are carried out. Reference "A" stands for the begin of the experiment and "B" is used once the solution has been renewed (experiments VIII–XII). For instance, glass powder in experiment VIII was first leached in pure water for 46 days at the conditions indicated in Table 3 under the label "VIIIA"; the leaching solution was then renewed with a 200 ppm calcium solution and the experiment reference becomes VIIIB. The same procedure was followed for experiments IXA/B and XA/B but this time the renewal solution was a 1000 ppm calcium solution for experiment IXB and pure water for experiment XB. Therefore experiments VIIIA, IXA and XA are performed in initially pure water as experiment I is.

In order to study the protective properties of the passivating reactive interphase (PRI)—especially in terms of solid state interdiffusion—transient alteration states must be excluded. This can be achieved initially by enriching in silica the reacting solution to limit network hydrolysis, allowing a homogeneous passivating interphase to be formed from the very beginning of glass alteration. A minimum silicon concentration of 100 ppm was therefore chosen, in agreement with the concentrations generally observed during the alteration of the Si B Al Na Zr glass in initially pure water at 90 °C, for a S/V ratio of 80 cm^{-1} and pH 8.7.

All experiments were carried out in a static system in 120 or 180 mL PTFE reactors. MilliQ water (18.2 MΩ cm at 25 °C) was used for all solutions. For the second set of experiments (Table 4), the solution was degassed under strong stirring and Ar bubbling (through a scrubbing flask filled with a molar sodium hydroxide solution) for 4 hours inside a glovebox also under Ar atmosphere. These precautions were taken in order to lower the carbon dioxide content during the experiments and thus minimize the formation of $CaCO_3$. Furthermore, silicon solutions were prepared by dissolving amorphous silica at neutral pH at 90 °C and their concentrations were checked by Spectroquant® analysis with a UV–vis spectrophotometer. Calcium concentrations were obtained by dilution of a concentrated $CaCl_2$ solution and also checked by a photometric method.

Table 2
Data for the different powder batches. Powder batch number 2 washing was less effective compared to the others and shows a higher specific surface area due to some small particles remaining in the sample.

Powder batch	1	2	3	4
Particle size (μm)	40–100	40–100	40–100	40–100
Specific surface area ($m^2\ g^{-1}$)	0.0633 ± 0.0005	0.1285 ± 0.0005	0.0870 ± 0.0005	0.0752 ± 0.0002
Density ($g\ cm^{-3}$)[a]	2.427	2.427	2.427	2.427

[a] Measured with a hydrostatic balance.

Table 3
Study of the influence of the initial calcium concentration and solution renewal on glass alteration. Experiment numbers with a "B" suffix indicate samples previously leached in pure water (experiments initially labeled with a "A" suffix). For all experiments, temperature was 90 °C and pH 8.7 (90 °C).

Experiment number	Powder batch	S/V (cm^{-1})	C^0_{Ca} (ppm)
I	1	72	0
II	1	80	5
III	1	80	50
IV	2	80	100
V	2	80	200
VI	2	80	400
VII	2	80	600
VIIIA	1	80	0
VIIIB	1	80	200
IXA	3	55	0
IXB	3	55	1000
XA	3	55	0
XB	3	55	0

Solutions aliquots were taken at regular intervals over 6 months and pH was monitored and maintained at 8.7 ± 0.1 at 90 °C by addition of molar sodium hydroxide solution (8.7 ± 0.1 is the roughly constant pH measured at 90 °C in initially pure water experiments for a S/V ratio of 80 cm^{-1} between one and more than two thousand days). Prior to Inductively Coupled Plasma Atomic Emission Spectrophotometry (ICP-AES) measurement, all aliquots were ultrafiltered with a 3–4 nm pore size centrifugation cells and then acidified with nitric acid to reach a 0.5 M HNO_3 concentration.

Time-Of-Flight Secondary Ion Mass Spectroscopy investigations were performed on 3 cm^2 diamond-polished glass disks at Biophy Research Laboratory in Fuveau (France) on ION-TOF ToF-SIMS IV and V devices working with Ga and Bi analysis guns, respectively. One glass disk cut in four pieces was placed within the powder layer inside the PTFE reactors for all experiments described in Table 4. All glass elements were monitored as well as the calcium coming from solution. Time-Of-Flight SIMS is based on the production of charged species (secondary ions) which are detected and discriminated thanks to a TOF analyzer. The material is ionized by bombarding the surface with a primary ion source. Secondary ions are then extracted and accelerated with the same kinetic energy and sorted as a function of their time of flight, which varies with the square root of their mass-to-charge ratio. One of the main differences with conventional dynamic SIMS analysis is the primary Ga or Bi ion gun which is not used for sample abrasion but for analysis purposes and only induces moderate ionization of the surface due to the weak primary intensity. In order to carry out depth analysis, a second beam, the electron impact gun, is used with higher current intensity. Since the abrasion step and surface characterization are separated, the analysis of nanometric to 1 μm layer becomes possible with high mass and depth resolution. For insulating samples, such as glass, a flood gun is also required to neutralize the surface charge. In order to link abrasion time and altered thickness, the depth of the crater is measured by optical profilometer at the end of the analysis.

Table 4
Study of chemical depth evolution and solid state diffusion coefficients in the altered glass layer. Experiment numbers followed with an "A" suffix refer to the prior alteration step (70 and 77 days for experiments XIA and XIIA, respectively), and with a "B" after solution renewal. All these experiments were carried out in glovebox under Ar atmosphere. The temperature was 90 °C, S/V 80 cm^{-1} and pH 8.7 (90 °C).

Experiment number	Powder batch	C^0_{Si} (ppm)	C^0_{Ca} (ppm)
XIA	4	0	0
XIB	4	0	>1000
XIIA	3	>100	0
XIIB	3	>100	>1000
XIII	4	0	200
XIV	3	>100	200

SEM observations were performed for almost every experiment. The observed alteration layers don't exhibit typical morphologies related to precipitates of crystallized hydrated calcium silicate.

3.2. Calculation method

Based on the ICP-AES concentrations, corrected for the HNO_3 dilution factor, the equivalent alteration thickness in element i, noted e_i is calculated by integrating Eq. (1).

$$\frac{d(e_i)}{dt} = \frac{d\left(\frac{C_i}{S/V x_i \rho}\right)}{dt} \quad (1)$$

where S/V is the glass-surface-area-to-solution–volume ratio (m^{-1}), C_i is the concentration in element i ($g\ m^{-3}$), x_i is the mass fraction of element i in the glass (–), ρ is the glass density ($g\ m^{-3}$) and t the time (d). This expression is also equal to the alteration rate of element i, r_i (2).

$$r_i = \frac{d(e_i)}{dt} \quad (2)$$

Due to glass alteration, aliquot sampling and solution evaporation, the S/V ratio and C_i are obviously not constant in time and equivalent alteration thicknesses must be calculated iteratively with Eq. (3). Thus, for a sample taken at time t, the equivalent thickness will be equal to the previous value at $t-1$ plus the variation during the interval.

$$(e_i)_t = (e_i)_{t-1} + \Delta(e_i) = (e_i)_{t-1} + \frac{C_i^t - C_i^{t-1}}{(S/V)_i x_i \rho} \tag{3}$$

The solution volume can be easily monitored by weighing all the aliquots and the PTFE reactors before and after each experimental step. Concerning the glass surface area, a spherical model was considered in order to take into account powder shrinkage during the experiment.

The percentage of altered glass, $AG\%$, can be therefore expressed as follows in terms of R_t and the initial radius, R_0:

$$\left.\begin{array}{l} V_t = \frac{4}{3}\pi \cdot R_t^3 \\ V_0 = \frac{4}{3}\pi \cdot R_0^3 \end{array}\right\} AG\% = \frac{V_0 - V_t}{V_0} = 1 - \frac{V_t}{V_0} = 1 - \frac{R_t^3}{R_0^3} \tag{4}$$

From Eq. (4), it is then possible to establish the evolution of the equivalent alteration thicknesses e_t at a given time t (Eq. (5)).

$$e_t = R_0 - R_t = \left(1 - (1 - AG\%)^{1/3}\right) R_0 \tag{5}$$

It's important to note that R_0 is not determined with the particle size given in Table 2, but by considering the glass density ρ and its specific surface area SSA as expressed in Eq. (6). The glass particles are modeled as perfect spheres developing the same specific surface area as the glass grains but having smaller diameters than expected from grounding.

$$R_0 = \frac{3}{\rho \cdot SSA} \tag{6}$$

$AG\%$ can be assessed from the boron solution analysis by iteratively calculating the leached fraction without omitting all mass losses due to sampling. Boron is usually chosen for such calculations because this element is not retained in secondary phases and is one of the first leached components (Scheetz et al., 1985). This approach leads to Eq. (7).

$$\begin{aligned} AG\% &= \frac{m_{boron}^{leached}}{m_{boron}^0} = \frac{m_{boron}^{leached}}{m_{glass}^0 \cdot x_{boron}} \\ &= \frac{C_{boron}^t \cdot V^t + \sum_{i=1}^{t-1} C_{boron}^i \cdot V_{aliquot}^i}{m_{glass}^0 \cdot x_{boron}} \end{aligned} \tag{7}$$

Finally, in solutions with aqueous silica concentration near glass apparent equilibrium concentration, namely when the glass alteration rate is no longer driven by matrix hydrolysis but rather by interdiffusion mechanisms, diffusion coefficients can be assessed with the help of Fick's second law (Crank, 1975; Chave et al., 2007). Here, the assumption of a semi-infinite medium implies that the PRI thickness increases according to the square root of time as described in Eq. (8)

$$e_{boron} = (1 - (1 - AG\%)^{1/3}) R_0 = \frac{2}{\sqrt{\pi}} \sqrt{D_{boron}^{Fick} \cdot t} \tag{8}$$

4. RESULTS

4.1. Effect of calcium concentration

The effect of the calcium concentration on calcium-free fresh glass behavior (experiments I–VII) was investigated based on boron release and compared with alteration in initially pure water as shown in Fig. 2(a) and (b). From Fig. 2(a) and (b), the average alteration rates can be determined leading to Fig. 3. Thus it can be shown that enough calcium available from solution can strongly reduce the glass alteration kinetics compared with the pure water experiment.

Calcium consumptions in solution are also plotted in Fig. 4 for experiments with initially 5/50/100 and 200 ppm of calcium (experiments II–V). Below an initial concentration of 100 ppm all the calcium supplied by the solution is consumed.

4.2. Pre-altered sample and solution renewal

Experiments VIIIB to XB are a continuation of the study of the effect of the calcium concentration on glass alteration. In previous experiments I–VII, a fresh glass sample was tested and a drastic effect on glass alteration was observed when the calcium concentration was below a given range (50–100 ppm). New investigations were carried out on samples previously altered for 1 month in pure water with solution renewal in order to study the calcium consumption under those conditions (experiments VIIIB–XB). Concerning solution renewal, it was preferred to keep a small amount of solution rather than taking the risk to dry the sample. Therefore a very small amount of pre-alteration solution was not removed before solution renewal for the Ca 200 ppm experiment (experiment VIIIB). This induced a calculated initial boron equivalent thickness around 60 nm which was corrected only on Fig. 5 for the reader‘s convenience. Boron equivalent thicknesses are given in Fig. 5 with alteration rates in Table 5. These results clearly show that the calcium concentration required to see an effect on the glass alteration is much higher for a pre-altered sample (1000 vs. 100 ppm). These results are confirmed by the calcium consumption plotted in Fig. 6 for two initial calcium concentrations of 200 and 1000 ppm (experiments VIIIB and IXB).

4.3. Experiments under controlled atmosphere and solid state characterization

Further experiments were then carried out under Ar atmosphere with glass disks, within the PTFE reactors, for solid state characterization. The evolution of the altered glass percentage for different solution compositions in contact with fresh glass are plotted in Fig. 7 (experiments XIA/XIIA/XIII and XIV). These results confirm the behavior observed with experiments I–VII (Fig. 2) and the major effect of the added calcium on the rate drop. Alteration rates and diffusion coefficients were determined, according to the previously described calculation method for each experiment and summarized in Table 6. Examples of square root

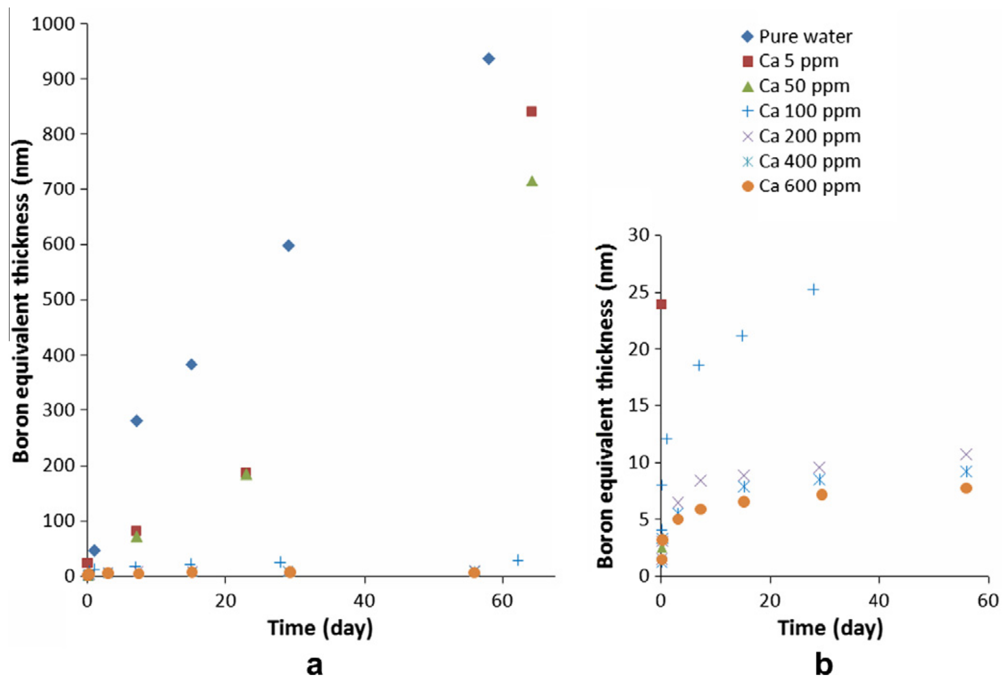

Fig. 2. (a) and (b) Effect of the Ca concentration in solution on the glass alteration behavior at pH 8.7, 90 °C and 80 cm^{-1}. Initial calcium concentrations are given in caption and refer to experiments I–VII. (b) is a close-up on low boron equivalent thicknesses of the (a).

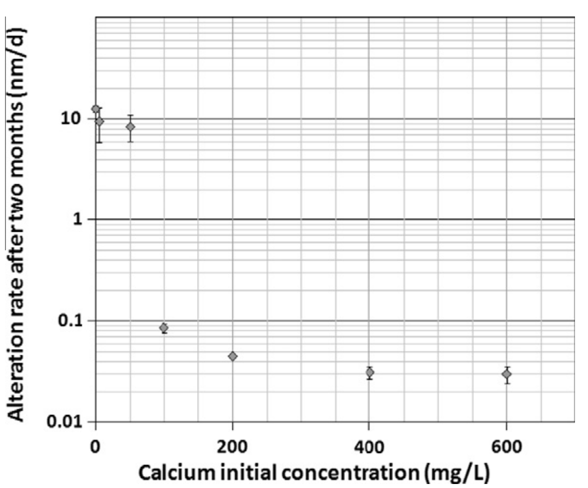

Fig. 3. Alteration rates after 2 months as a function of the initial calcium concentrations (Si B Na Al Zr glass, pH 8.7, 90 °C, 80 cm^{-1}). Kinetic values were calculated by linear regression of the last three points of Fig. 2(a) and (b) for experiments I–VII.

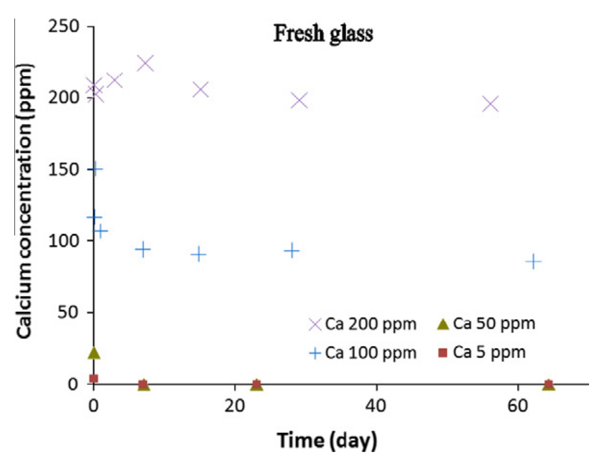

Fig. 4. Evolution of the calcium concentration in solution for different initial concentrations with a fresh glass at pH 8.7, 90 °C and 80 cm^{-1}. Initial calcium concentrations are given in caption and refer to experiments II–V (calcium concentration from 5 to 200 ppm, respectively).

of time evolution of boron concentrations are shown in Fig. 8.

After a 70 or 77 day pre-alteration step in pure water (experiments XI) and silica rich solution (experiments XI and XII), experiments underwent a solution renewal with calcium-enriched solution. During this operation the glass powder was not rinsed and a dead volume of solution of 10–15 mL remained in the PTFE reactors. Here, this dead volume induced relatively high initial concentrations compared to the low alteration rate observed in calcium-enriched solutions. The concentration evolutions for experiments XIA/B and XIIA/B are given in Figs. 9(a)/(b) and 10(a)/(b), respectively.

Contrary to the previous experiments, the boron concentrations after solution renewal could not be used to determine the alteration rates and diffusion coefficients. In fact, the boron concentration variation over time was not readily discriminated from the remaining concentration of the diluted dead volume.

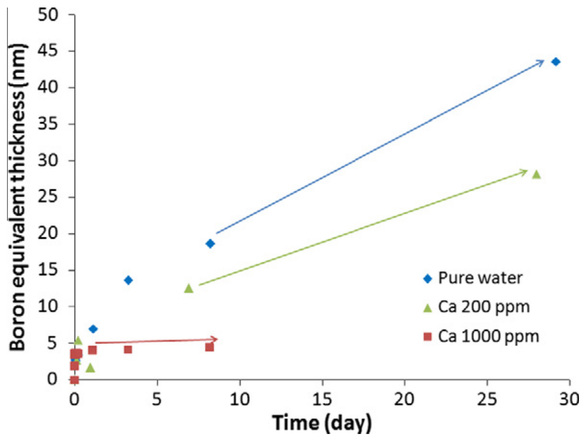

Fig. 5. Boron equivalent thicknesses of glass sample pre-altered for 1 month in pure water before calcium enriched solution renewal at 90 °C, pH 8.7 and 80 cm^{-1} (200 ppm: experiment VIIIB) and 55 cm^{-1} (1000 ppm: experiment IXB) or in pure water (experiment XB). It has to be said that a small amount of pre-alteration solution was not removed before solution renewal for the Ca 200 ppm experiment inducing a calculated initial boron equivalent thickness around 60 nm which was corrected on the figure. Solution renewal conditions are given in caption.

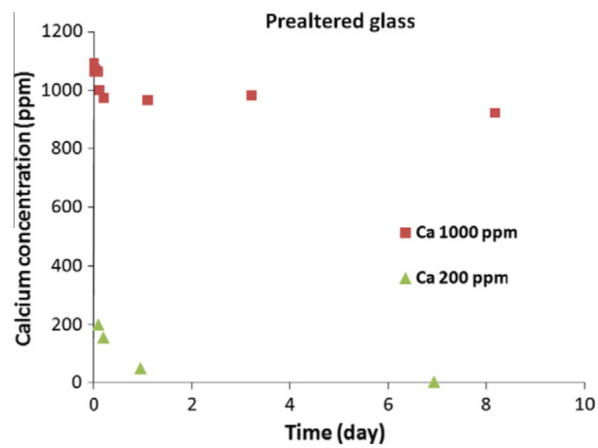

Fig. 6. Ca-rich solution renewal after alteration in pure water for 46 days at pH 8.7, 90 °C and 55 cm^{-1} (1000 ppm Ca: experiment IXB) or 80 cm^{-1} (200 ppm Ca: experiment VIIIB).

Table 5
Observed alteration rates for the pure water pre-altered sample experiments.

Experiment number	C^0_{Ca} (ppm)	Alteration rate (nm d^{-1})
VIIIB	200	0.76 (between 7 and 28 days)
IXB	>1000	0.06 (between 1 and 8 days)
XB	0	1.19 (between 8 and 29 days)

Nevertheless, thanks to the experimental care taken for this set of experiments, all the glass pellets were characterized by TOF-SIMS analysis especially those subjected to solution renewal (experiments XI and XII), this should allow the characterization of the calcium signal over a larger thickness. Two examples of chemical depth analysis of glass pellets are given in Fig. 11(a) and (b) for experiments XIB and XIII, respectively. The high sensitivity of TOF-SIMS made it possible to detect the presence of potassium contamination, certainly due to pH electrode solution leakage in our samples, as shown in Fig. 11(b).

5. DISCUSSION

5.1. Effect of calcium concentration

Figs. 2 and 3 demonstrate that the presence of calcium in solution induces a strong decrease in the glass alteration rate. For Ca concentrations equal or below 50 ppm, only a slight effect compared with pure water experiments (I–III) is observed on the alteration rate. In these conditions, calcium concentration in solution drastically decreases and after few days the remaining calcium concentration in solution is very close to detection limit for experiments II and III. With such low calcium concentrations, alteration kinetic is high and hydrated surface layer thickness is the same than in pure water experiment (Fig. 3). Calcium concentration decrease is explained by calcium reactivity with the silica network of this hydrated surface layer. On the other hand, when calcium concentration is above 50–100 ppm (experiments IV–VII), the altered thickness after 58 days is reduced by a factor of ~30 compared with the experiment without calcium (experiment I). In Fig. 4, it can be seen that high initial Ca concentrations (experiments IV–VII) does not decrease significantly and reaches a plateau. Obviously, one part of the calcium in solution is meant to react with the uprising hydrated surface layer. However, initial calcium concentrations are so high in experiments (V–VII) that calcium decrease is hardly measurable. Nevertheless, a calcium decrease is indeed observed for experiment (IV), case of 100 ppm of calcium.

From calcium concentrations (Fig. 4) and boron release rate (Fig. 3), it can be concluded that significantly high Ca concentration in solution, typically between 50 and 100 ppm, is required to form a highly passivating reactive interphase. In these conditions, the hydrated surface layer growth rate is drastically lessened, compared to experiments in pure water or with lower calcium concentration, and the aqueous calcium consumption due to the reaction with the silica network is therefore reduced.

The hydrated surface layer is a complex medium. Due to aluminum and zirconium low solubility, an Al, Zr and Si rich hydrated layer can form even far from Si steady state in solution. This layer does not exhibit passivating properties because of its low Si content. However, it can still be reactive and consume calcium from solution.

Therefore, the calcium concentration between 50 and 100 ppm required for observing a strong decrease in the alteration rate could be dependent or even proportional to the amount of non passivating Al and Zr rich hydrated layer which is formed before Si steady state is reached in solution. Consequently, the observed transition zone between 50 and 100 Ca ppm is only relevant for fresh glass and the surface area to solution volume ratio of these

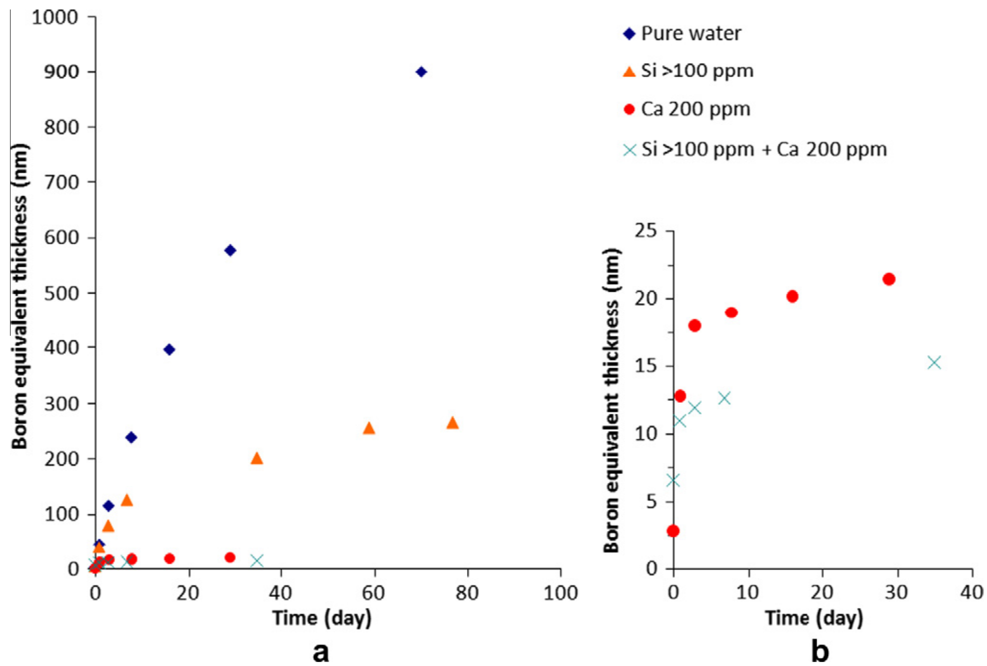

Fig. 7. (a) and (b) Comparison of boron equivalent thicknesses for various solution compositions under controlled atmosphere in presence of glass pellets at pH 8.7, 90 °C and 80 cm^{-1}. Initial conditions are given in caption and refer to experiments XI1 (pure water), XIIA (Si > 100 ppm), XIII (Ca 200 ppm) and XIV (Si > 100 ppm + Ca 200 ppm). (b) is a close up on the low boron equivalent thicknesses of (a).

Table 6
Glovebox experiment alteration rates and boron diffusion coefficients D_B at pH 8.7, 90 °C and 80 cm^{-1}. Square correlation coefficients R^2 for the determination of D_B are also given in this table and examples of square root of time evolution are shown in Fig. 8.

Experiment number	C^0_{Si} (ppm)	C^0_{Ca} (ppm)	Alteration rate (nm d^{-1})	D_B ($m^2\ s^{-1}$)	R^2
XIA	0	0	7.9 (between 29 and 70 days)	1.3 ± 0.110^{-19}	0.9981
XIIA	>100	0	1.6 (between 35 and 77 days)	$7.0 \pm 1.1 \times 10^{-21}$	0.9873
XIII	0	200	0.12 (between 8 and 29 days)	$1.4 \pm 0.2 \times 10^{-23}$	0.9919
XIV	>100	200	0.09 (between 7 and 35 days)	$6.5 \pm 0.7 \times 10^{-24}$	0.9931

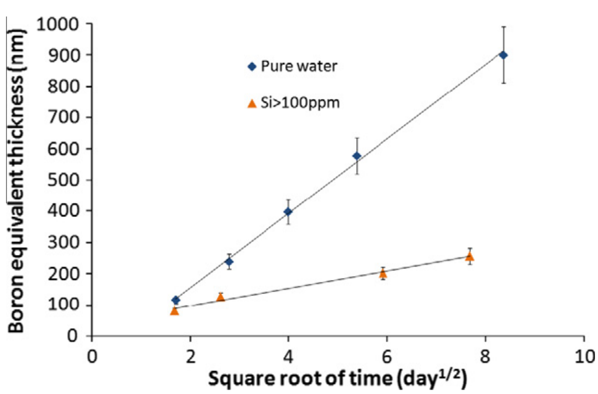

Fig. 8. Evolution of the boron equivalent thickness versus the square root of time for the experiments in silicon-enriched solution and pure water at 90 °C, pH 8.7 and 80 cm^{-1} (experiment XIIA and XIA, respectively).

experiments. Therefore experiments on pre-altered samples were designed in order to validate this hypothesis.

5.2. Pre-altered sample and solution renewal

When the glass powder was previously altered in pure water and then subjected to solution renewal with a 200 ppm Ca solution, no significant decrease in the alteration rate could be observed (experiment VIIIB). Moreover, under these conditions the calcium concentration in solution decreases very quickly as shown in Fig. 6. From experiment VIIIB it can be concluded that in the case of a pre-altered glass specimen, higher calcium concentration are necessary to obtain a significant decrease in the glass alteration rate. For instance, with an expected ~700 nm thick amorphous alteration layer following a 46-day prior alteration step in pure water at 90 °C, pH 8.7 and 80 cm^{-1}, a higher Ca concentration (~1000 ppm) is required (Fig. 5 and Table 5). This demonstrates that calcium consumption is dependent on the amount of hydrated surface layer formed before Si steady state in solution is achieved and a Si and Ca rich passivating reactive interphase can form.

Previous experiments on the French reference nuclear glass showed no significant effect of calcium addition on

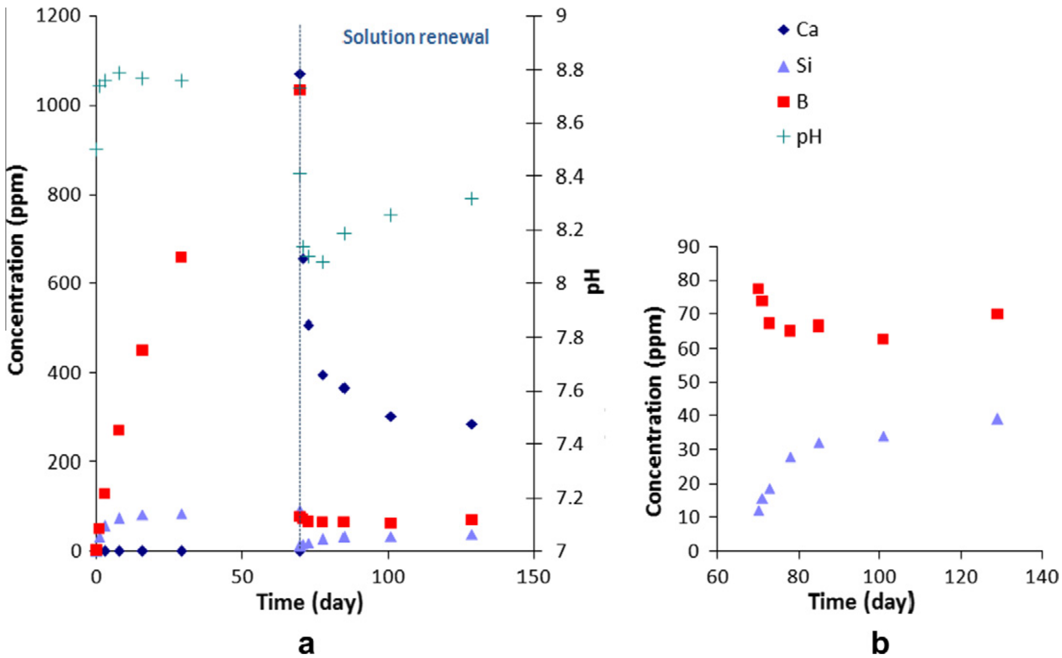

Fig. 9. (a) and (b) Concentration evolutions in time for a pure water pre-altered sample (experiment XIA) with calcium-rich solution renewal at 90 °C, 80 cm^{-1} and pH 8.7 (experiment XIB). Solution renewal was carried out after 70 days. (b) is a close up on the low concentration values of (a) after solution renewal.

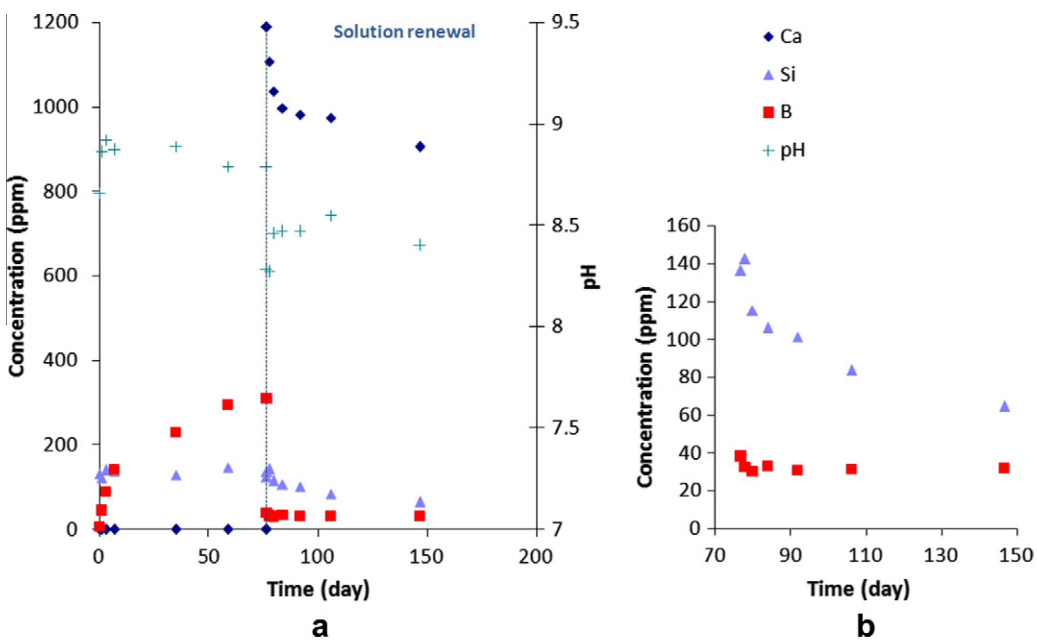

Fig. 10. (a) and (b) Concentration evolutions in time for a pre-altered sample in silica-enriched solution (experiment XIIA) with calcium + silicon solution renewal at 90 °C, 80 cm^{-1} and pH 8.7 (experiment XIIB). Solution renewal was carried out after 77 days. (b) is a close-up on the low concentration values of (a) after solution renewal.

the initial alteration rate (Gin et al., 1995). The role of calcium on the glass leaching behavior seems to be observed only when a passivating reactive interphase (PRI) is formed, i.e. when Si steady state is reached in solution. This suggests that calcium from the solution is incorporated in the PRI during the glass leaching, but this hypothesis could not be confirmed by depth profile analysis since no glass disk was added in this experiment. Moreover, the presence of carbon dioxide could induce the formation of calcite that not only decreases the quality of depth profile analysis by enhancing the surface roughness, but could also skew our understanding of the calcium localization in our samples.

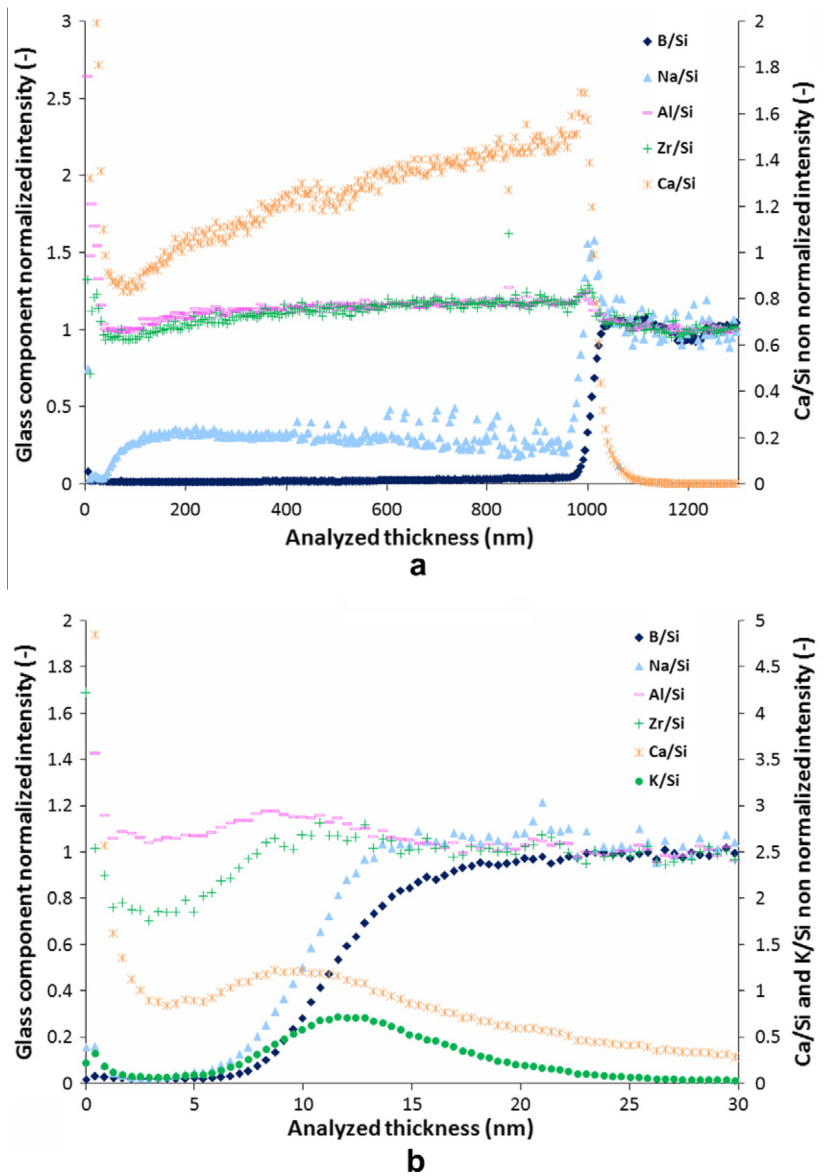

Fig. 11. (a) TOF-SIMS analysis on a glass pellet pre-altered in pure water for 77 days with 1000 ppm calcium enriched solution renewal during 8 months at 90 °C, 80 cm^{-1}, pH 8.7 (experiment XIB). For comparison, boron equivalent thickness obtained from ICP-AES analysis is around 900 nm. (b) TOF-SIMS analysis on a glass pellet altered in 200 ppm calcium-rich solution for 9 months at 90 °C, 80 cm^{-1}, pH 8.7 (experiment XIII). For comparison, boron equivalent thickness obtained from ICP-AES analysis is around 30 nm.

A second series of experiments (XI–XIV) was therefore carried out in CO_2-free atmosphere and this time with glass disk in addition of the powder.

5.3. Experiments under controlled atmosphere

Fig. 7 confirms the initial conclusions. Under these conditions, diffusion coefficients were obtained with values ranging from 10^{-19} to 10^{-24} $m^2\,s^{-1}$, typical of a solid-state diffusion mechanism. The results for the boron alteration rates and the diffusion coefficients are calculated from the values given in Table 6 and compared in Table 7.

These results show that silicon addition near the glass equilibrium value at pH 8.7 and 90 °C induced an expected decrease in the alteration rate. In fact, a factor 5 alteration rate decrease was measured between alteration in the Si-enriched solution and in pure water. Nevertheless, it appears that the silicon saturation effect was significantly smaller than the one observed with calcium, which at 200 ppm induced a rate drop by a factor 68. Noteworthy, in the presence of both calcium and silicon, a further effect could be observed with an alteration rate 84 times lower compared to pure water experiment. Actually, the main effect is driven by the presence of calcium, even if it seems to be slightly enhanced by the addition of silicon. Concerning the diffusion coefficients, the comparison suggests that the pure water experiment is not driven only by interdiffusion mechanisms insofar as, in that case, hydrolysis plays a sizeable role at the very beginning of the alteration. On the other hand, experiments XII and XIV can be directly compared since their initial Si-saturated conditions minimized the hydrolysis part of the leaching. Calcium addition causes the measured reactive diffusion coefficient to drop by four orders of magnitude based on boron release. Noteworthy, resulting values are even lower than diffusion coefficients observed in the case of the French reference nuclear glass altered in silica-rich solution at the same temperature and pH (Chave et al., 2007).

5.4. Solid state characterization and amorphous alteration layer composition determination

First of all, TOF-SIMS analysis allowed the comparison of the altered thicknesses estimated by both solution analysis and solid state characterization. Altered thickness, around 1 μm, obtained from Fig. 11(a) is in good agreement with the boron equivalent thickness estimated to 900 nm by ICP-AES analysis. On the other hand, for the sample altered in calcium rich solution shown in Fig. 11(b), the thicknesses obtained by TOF-SIMS (12–15 nm) and ICP-AES analyses (30 nm) are not in good agreement since (i) the abrasion rate was not determined directly on this sample but on a silicon rich pre-altered sample and (ii) the analysis was carried on well beyond the amorphous alteration layer – fresh glass interface making the determination of the real altered layer thickness less precise.

Considering experiment XI which consists in a first alteration step in pure water (experiment XIA) followed by a solution renewal in calcium enriched solution (experiment XIB) it can be seen, according to ICP-AES solution analysis, that a 900 nm thick altered layer is formed during the alteration in pure water for 77 days (Table S2). After this pre-alteration step, the solution was renewed with a calcium enriched solution for 8 further months in the same conditions at 90 °C, pH ~8.7. Depth profile of the pellet altered 77 days in pure water and 8 months in 1000 ppm Ca solution shown on Fig. 11(a), highlights that the calcium is actually strongly embedded within the amorphous alteration layer formed during the alteration step in pure water. After solution renewal, it can also be noticed that the glass alteration rate strongly decreases compared to previous pure water conditions (Fig. 9(b)). Calcium incorporation within the amorphous alteration layer can also be observed when fresh glass is leached in calcium-enriched solution (200 ppm) without any pure water pre alteration step (experiment XIII) as shown in Fig. 11(b). In that case, calcium can be incorporated within the amorphous alteration layer since the very beginning of the water-glass interaction leading to the formation a very thin layer even after 9 months of alteration at 90 °C, pH ~8.7. The difference in layers thicknesses between experiments (XI and XIII) is due to the prealteration step in pure water. Furthermore, ICP-AES analysis confirms that the aqueous Ca^{2+} concentration decreases in time as shown in Fig. 6. Since no secondary crystallized phases were observed by SEM analysis on the glass surface, this result clearly indicates that the calcium is incorporated in the amorphous alteration layer. Calcium evolution in time is not steady and shows a sharp initial drop followed by an asymptotic trend. If we consider the experiments with a pre alteration step in pure water (experiment XI) or in silicon enriched solution (experiment XII), it can be seen that the magnitude of the calcium concentration drop at the very beginning of the calcium enriched solution renewal increases with the thickness of the amorphous layer formed during the pre alteration step (which is around 900 nm for experiment XI and 300 nm for experiment XII). Similarly, it is important to recall that the pH was adjusted to 8.7 (90 °C) at regular intervals thanks to 1 M NaOH addition. Considering the solution renewal experiments, a pH drop of 0.2–0.6 unity can be noted between each sampling operation. For experiment XII, the total amount of sodium hydroxyde added within the system in order to maintain the pH_{90} at 8.7 was around 1.6 mmol. In comparison, the calcium concentration drop observed in this experiment implies a 0.9 mmol calcium consumption .This solution acidification is therefore consistent with the calcium consumption and with its incorporation within the amorphous layer by the following mechanism:

$$\equiv Si-OH + Ca^{2+} + HO-Si\equiv \longrightarrow \equiv Si-O-Ca-O-Si\equiv + 2H^{+} \quad (9)$$

Table 7
Comparison of diffusion coefficients and alteration rates for glovebox experiments. For instance, alteration rate in pure water is five times higher than in silicon-saturated solution. Similarly, the diffusion coefficient in presence of calcium and silicon is three orders of magnitude lower than for the same experiments with added silicon alone.

A / B	XI A water	XII A Si	XIII Ca	XIV Si+Ca
XI A water	1	5	68	84
XII A Si	19	1	13	16
XIII Ca	9300	500	1	1.2
XIV Si+Ca	20000	1100	2.2	1

Alteration kinetic ratio: B/A

Diffusion coefficient ratio: A/B

The same reaction was proposed to explain the interaction of silica glass with calcium hydroxide by (Armelao et al., 2000). In addition, it was seen by TOF-SIMS that the solid-state calcium profile appears to be constant within most of the altered layer. This is actually a sign of chemical incorporation, otherwise a profile similar to that of potassium, which is not a glass component, would have been observed (Fig. 11(b)). In fact, the potassium analysis shows a bell shaped profile centered on the fresh glass/amorphous alteration layer interface without any specific integration within the layer. Finally, thanks to ICP-AES solution analysis, it is possible to determine the amount of Ca incorporated in the layer and thus quantify the mean elemental ratios such as Si/Ca, Al/Ca and Zr/Ca in the solid phase. This approach was applied for all leaching experiments in presence of calcium; the results are summarized in Table 8.

According to Table 8, for all the experiments carried out with an adequate amount of calcium provided by the solution, namely for which calcium plays a role in the kinetic drop, the initially calcium-free layers evolve toward the same composition domain. If calcium was incorporated in the amorphous alteration layer exclusively as a charge compensator the (1/2Al + Zr)/Ca elemental ratio should be 1 since Al and Zr are respectively under AlO_4^- and ZrO_6^{2-} forms within the glass. Here the average composition domain gives a value of 0.8 which means that more calcium is integrated within the amorphous layer than needed for Al and Zr charge compensation. This observation is relevant to Eq. (9) and confirms that calcium in solution should be retained in this way even in contact with a pure silica alteration layer.

Another interesting point is to compare these values to the amorphous alteration layer molar ratios obtained from a French reference nuclear glass leaching experiment in which calcium was already incorporated in the glass structure. In that case, the Si/Ca, Al/Ca and Zr/Ca molar ratios were 10.54, 1.33 and 0.3, respectively. These values are quite close, but this is not surprising and can be explained insofar as these elements are strongly retained within the altered layer during leaching. Nevertheless, achieving the same molar ratio with an element provided by the solution highlights the amorphous alteration layer's reactivity toward the solution. This high reactivity is also revealed by the four orders of magnitude decrease in the diffusion coefficient. This behavior is certainly due to greater network connectivity and structure reorganization in the presence of calcium (Eq. (9)). Finally, this study also shows that modeling glass reactivity cannot be done by only taking into account the glass components but should also carefully consider the solution composition and the PRI reactivity toward. This remark is consistent with the modeling approach developed in Oelkers et al. (2009) stating that the accurate modeling of multi-oxide surface chemistry requires provision for the changing number and composition of surface sites.

Table 8
Altered surface layer component molar ratio in presence of calcium.

Experiment	Si/Ca	Al/Ca	Zr/Ca
XIII: Ca	8.25	1.5	0.33
XIV: Si + Ca	8.5	1.1	0.24
XIB: Ca renewal	8.0	1.0	0.23
XIIB: Si + Ca renewal	7.5	1.0	0.20

5.5. Understanding the role of calcium on transport properties within the PRI

The present experiments evidence the calcium effect on PRI transport properties. Nevertheless, the underlying molecular mechanisms are still poorly understood. A literature survey on calcium-silica reactions gives interesting directions for understanding the process from both a thermodynamic and kinetic standpoint.

The calcium reaction with silica surfaces is highly pH-dependent. At $pH_{90°C}$ below 7, calcium is not expected to react with silica amorphous layers. On the other hand, for $pH_{90°C}$ above 10, hydrated calcium silicate precipitation is expected. Extensive literature is available on these calcium silicate hydrates due to their importance in cements (Sugiyama and Fujita, 2006; Richardson, 2008). Nevertheless, at slightly alkaline pH, i.e. when $pH_{90°C}$ is close to 9 and the Ca/Si ratio below 0.5, few studies are available concerning silica–calcium condensation of amorphous compounds. Consequently, precise geochemical modeling at these pH values is still necessary, as suggested by Frugier et al. (2009). The objective would be a quantitative description of calcium condensation in the hydrated surface layer (reaction (9)). This should be followed by en attempt to make the link between PRI composition and transport properties.

However besides "simple" thermodynamic an other effect of calcium might not be neglected: calcium has been identified as one of the most effective cations for catalyzing silica condensation. Nieto et al. (1995) proposed that the formation of silica bonds is induced by calcium ions in two steps. First, the calcium ion forms a bond with one silicate specie, which contains one ionized silanol (SiO^-), as illustrated in reaction (10).

$$\equiv Si{-}O^- + Ca^{2+} \longrightarrow \equiv Si{-}O{-}Ca^+ \qquad (10)$$

In the second step, this positive charge attracts a second silicate specie, forming an intermediate complex, which contains a bridge between two different silicate species induced by calcium ions. This unstable complex leads to the formation of a siloxane bond by ejecting calcium ion as illustrated in reaction (11).

$$\equiv Si{-}O{-}Ca^+ + {}^-O{-}Si\equiv + H_2O \xrightarrow{\equiv Si-O-Ca-O-Si\equiv} \equiv Si{-}O{-}Si\equiv + Ca^{2+} + 2OH^- \qquad (11)$$

These two reactions show the enhancing action of calcium ions on the formation of the siloxane bond and explain that both high pH and high calcium concentrations can enhance the silica condensation kinetics. In Gaboriaud et al. (1999, 2002, 2005), the mechanism of gelation and the structural features of the final gel are characterized versus the nature of the alkali ions, the calcium concentration, and the hydroxide ion content. They observed that "the only important parameter determining the relevant structural features of the gels was calcium concentration". This investigation demonstrates that the concentration of calcium ions is the main factor that controls aggregation and gelation processes in alkali-silica solutions. In fact, solutions with a high calcium concentration yield gels composed of rather small fractal aggregates and large particles formed just after calcium addition. On the other hand, solutions with low calcium content induce the formation of gels mainly composed of large fractal aggregates coexisting with small primary silicate species.

Consequently, there is evidence suggesting that both the condensation kinetics and amorphous alteration layer structure are modified by calcium that does not necessarily belong to the layer composition. However, in our study, calcium is incorporated in the hydrated surface layer and there is no evidence of reaction (11). Since incorporation of calcium induces a drastic change of the hydrated surface layer composition, a strong modification of its passivation properties is therefore all the more understandable. Nevertheless, the mechanisms proposed by Nieto et al. (1995) is not to be excluded when trying to make the link between PRI composition and PRI passivation properties. Experimental and theoretical work certainly remains to be done in this area for a better understanding of calcium effect and for knowing whether or not theses mechanisms could be generalized to other alkaline earth (Ba, Mg) (Berger et al., 1987).

6. CONCLUSIONS

This work brings new and fundamental evidence toward understanding how the hydrated surface layer controls synthetic glass dissolution kinetics: The hydrated surface layer is reactive with respect to the solution, it was proved to incorporate calcium available in solution (around a pH 90 °C near 9). Moreover, calcium rich hydrated layers are far more effective to passivate the glass than calcium free ones. The apparent reactive diffusion coefficient of solvated ions (boron and sodium) and water is four orders of magnitude lower when calcium is available in sufficient amounts, whether it comes from the glass or solution. These experiments provide new evidence of the role of condensation mechanisms in glass alteration: reactive interdiffusion of water and solvated ions proceed in a place which is highly sensitive to condensation processes. Predicting such a strong effect of calcium would have been almost impossible for most of the available glass alteration models who do not allow for the reactivity with solution of the hydrated surface layer which limits water diffusion. Can the phenomena observed for glass surfaces be generalized to multi-oxide minerals surfaces or to other alkaline earth? Further experimental evidence of the key role potentially played by condensation mechanisms could significantly enhance our understanding of multi-oxide mineral alteration kinetics.

ACKNOWLEDGEMENTS

The authors are very grateful to Associate Editor, Dr. Jacques Schott and to the reviewers especially Dr. Domenik Wolff-Boenisch for their careful editing and significant improvement of the manuscript.

APPENDIX A. EXPERIMENTAL DATA

Table S1 indicates the initial conditions and masses engaged in each experiment. On the other hand, final solution concentrations expressed in mg L^{-1} are listed in Table S2 with equivalent altered thicknesses, last pH value (or the previous one if written in *italic*) and altered glass percentages calculated as described in the "calculation method" section. It should be noted that sodium concentrations are raw values which are not refined for the amount of Na coming from NaOH additions for pH adjustments. Missing values are replaced by "–", whereas "X" stands for meaningless calculations and "<QL" for concentrations below the quantification limit. For instance, when silicon is added in the system, the resulting silicon altered thickness has to be corrected for the initial Si concentration. This approach is not always possible due to analysis accuracy limitations; in such cases the result is not given and is marked with an "X".

REFERENCES

Advocat T., Crovisier J.L., Clement A., Gerard F. and Vernaz E. (1995) Modeling of solution renewal with the KINDIS code: Example of R7T7 glass dissolution at 90 °C. In *Scientific Basis for Nuclear Waste Management XVIII* (eds. T. Murakami and R. C. Ewing). Mater. Res. Soc. Vol. 353, pp. 31–38.

Armelao L., Bassan A., Bertoncello R., Biscontin G., Daolio S. and Glisenti A. (2000) Silica glass interaction with calcium hydroxide: a surface chemistry approach. *J. Cult. Herit.* **1**, 375–384.

Berger G., Schott J. and Loubet M. (1987) Fundamental processes controlling the first stage of alteration of a basalt glass by seawater: an experimental study between 200° and 320 °C. *Earth Planet Sc Lett.* **84** (4), 431–445.

Bourcier W.L., Pfeiffer D.W., Knauss K.G., McKeegan K.D. and Smith D.K. (1990) A Kinetic model for borosilicate glass dissolution affinity of a surface alteration layer, In *Scientific Basis for Nuclear Waste Management*, Mat. Res. Soc. Symp. Proc. Vol. 176, pp. 209–216.

Bunker B. C. (1994) Molecular mechanisms for corrosion of silica and silicate glasses. *J. Non-Cryst. Solids* **179**, 300–308.

Bunker B. C., Tallant D. R., Headley T. J., Turner G. L. and Kirkpatrick R. J. (1988) The structure of leached sodium borosilicate glass. *Phys. Chem. Glasses* **29**(3), 106–120.

Cailleteau C., Angeli F., Devreux F., Gin S., Jestin J., Jollivet P. and Spalla O. (2008) Insight into silicate glass aqueous alteration mechanisms. *Nat. Mater.* **7**, 978–983.

Casey W. H., Westrich H. R., Banfield J. F., Ferruzzi G. and Arnold G. W. (1993) Leaching and reconstruction at the surfaces of dissolving chain silicate minerals. *Nature* **366**, 253–255.

Chardon E. S., Livens F. R. and Vaughan D. J. (2006) Reactions of feldspar surfaces with aqueous solutions. *Earth-Sci. Rev.* **78**, 1–26.

Chave T., Frugier P., Ayral A. and Gin S. (2007) Solid state diffusion during nuclear glass residual alteration in solution. *J. Nucl. Mater.* **362**, 466–473.

Conradt R. (2008) Chemical durability of oxide glasses in aqueous solutions: a review. *J. Am. Ceram. Soc.* **91**, 728–735.

Crank J. (1975) *The mathematics of diffusion* (Second edition). Oxford University Press.

Daux V., Guy C., Advocat T., Crovisier J. L. and Stille P. (1997) Kinetic aspects of basaltic glass dissolution at 90 °C: role of aqueous silicon and aluminium. *Chem. Geol.* **142**, 109–126.

Daval D., Martinez I., Corvisier J., Findling N., Goffé B. and Guyot F. (2009) Carbonation of Ca-bearing silicates, the case of wollastonite: experimental investigations and kinetic modeling. *Chem. Geol.* **265**, 63–78.

Doremus R. H. (1975) Interdiffusion of hydrogen and alkali ions in a glass surface. *J. Non-Cryst. Solids* **19**, 137–144.

Ferrand K., Abdelouas A. and Grambow B. (2006) Water diffusion in the simulated French nuclear waste glass SON 68 contacting silica rich solutions: experimental and modeling. *J. Nucl. Mater.* **355**, 54–67.

Frugier P., Gin S., Minet Y., Chave T., Bonin B., Godon N., Lartigue J. E., Jollivet P., Ayral A., De Windt L. and Santarini G. (2008) SON68 Nuclear glass dissolution kinetics: current state of knowledge and basis of the new GRAAL model. *J. Nucl. Mater.* **380**, 8–21.

Frugier P., Chave T., Gin S. and Lartigue J. E. (2009) Application of the GRAAL model to leaching experiments with SON68 nuclear glass in initially pure water. *J. Nucl. Mater.* **392**, 552–567.

Gaboriaud F., Nonat A., Chaumont D. and Craievich A. (1999) Aggregation and gel formation in basic silico–calco–Alkaline solutions studied: a SAXS, SANS, and ELS study. *J. Phys. Chem.* **103**, 5775–5781.

Gaboriaud F., Nonat A., Chaumont D. and Craievich A. (2002) Aggregation processes and formation of silico–calco–alkaline gels under high ionic strength. *J. Colloid Interf. Sci.* **253**, 140–149.

Gaboriaud F., Nonat A., Chaumont D. and Craievich A. (2005) Structural model of gelation processes of a sodium silicate sol destabilised by calcium ions: combination of SAXS and rheological measurements. *J. Non-Cryst. Solids* **351**, 351–354.

Geneste G., Bouyer F. and Gin S. (2006) Hydrogen–sodium interdiffusion in borosilicate glasses investigated from first principles. *J. Non-Cryst. Solids* **352**, 3147–3152.

Gin S., Godon N. and Vernaz E. (1995) Effect of inorganic aqueous species on the long term behavior of nuclear glass, In *Proceeding of the Fifth International Conference on Radioactive Waste Management and Environmental Remediation 2nd Ed. New York*, pp. 599–603.

Gin S. and Jegou C. (2001) Limiting mechanisms of borosilicate glass alteration kinetics: effect of glass composition. *Water–Rock Interact.* **279**, 282.

Gin S. and Jegou C. (2002) Theoretical review of the Aagaard–Helgeson law applied to the dissolution of minerals and glasses. *Chem. Geol.* **255**, 14–24.

Grambow B. and Muller R. (2001) First-order dissolution rate law and the role of surface layers in glass performance assessment. *J. Nucl. Mater.* **298**, 112–124.

Hellmann R. (1997) The albite-water system: Part IV. Diffusion modeling of leached and hydrogen-enriched layers. *Geochim. Cosmochim. Acta* **61**, 1595–1611.

Jegou C. (1998) Mise en évidence expérimentale des mécanismes limitant l'altération du verre R7T7 en milieu aqueux. Critique et proposition d'évolution du formalisme cinétique. Ph. D. thesis of Université Montpellier II.

Jegou C., Gin S., Vernaz E. and Larche F. (1999) Aqueous alteration kinetics of French R7T7 light water reference glass: simplified glass modeling approach. In *International Congress on glass XVIII. Am. Ceram. Soc.*

Jollivet P., Angeli F., Cailleteau C., Devreux F., Frugier P. and Gin S. (2008) Investigation of gel porosity clogging during glass leaching. *J. Non-Cryst. Solids* **354**, 4952–4958.

Lüttge A. (2006) Crystal dissolution kinetics and Gibbs free energy. *J. Electron. Spectrosc.* **150**, 248–259.

Muir I. J. and Nesbitt H. W. (1997) Reactions of aqueous anions and cations at the labradorite-water interface. Coupled effects of surface processes and diffusion. *Geochim. Cosmochim. Acta* **61**, 265–274.

Nieto P., Dron R., Thouvenot R., Zanni H. and Brivot F. (1995) Study by Ca-43 NMR spectroscopy of the sol-gel transformation of the calcium-silicate complex. *CR. l'Acad. Sci. Paris* **320**, 485–488.

Oelkers E. H. (2001) General kinetic description of multioxide silicate mineral and glass dissolution. *Geochim. Cosmochim. Acta* **65**, 3703–3719.

Oelkers E. H., Golubev S. V., Chairat C., Pokrovsky O. S. and Schott J. (2009) The surface chemistry of multi-oxide silicates. *Geochim. Cosmochim. Acta* **73**, 4617–4634.

Ojovan M. I., Pankov A. and Lee W. E. (2006) The ion exchange phase in corrosion of nuclear waste glasses. *J. Nucl. Mater.* **358**, 57–68.

Pokrovsky O. S. and Schott J. (2000) Forsterite surface composition in aqueous solutions: a combined potentiometric, electrokinetic, and speciation approach. *Geochim. Cosmochim. Acta* **64**, 3299–3312.

Rajmohan N., Frugier P. and Gin S. (2010) Composition effects on synthetic glass alteration mechanisms: Part 1. Experiments. *Chem. Geol.* **279**, 106–119.

Richardson I. G. (2008) The calcium silicate hydrates. *Cem. Concr. Res.* **38**, 137–158.

Scheetz B. E. et al. (1985) In *Scientific Basis for NUCLEAR WASTE MANAGEMENT VIII* (eds. C. M. Jantzen, J. A. Stone, and R. C. Ewing), Mater. Res. Soc. Vol. 44, pp. 129–134.

Schott J., Pokrovsky O. S., Spalla O., Devreux F. and Mielczarski A. (2002) The mechanism of altered layers formation on wollastonite revisited: a combined spectroscopic/kinetic study. *Geochim. Cosmochim. Acta* **66**, A686.

Spalla O., Barboux P., Sicard L., Lyonnard S. and Bley F. (2004) Influence of insoluble elements on the nanostructure of water altered glasses. *J. Non-Cryst. Solids* **347**, 56–68.

Sugiyama D. and Fujita T. (2006) A thermodynamic model of dissolution and precipitation of calcium silicate hydrates. *Cem. Concr. Res.* **36**, 227–237.

Van Iseghem P., Aertsens M., Gin S., Deneele D., Grambow B., McGrail P., Strachan, D. and Wicks G. (2007) A Critical Evaluation of the Dissolution Mechanisms of High-Level Waste Glasses in Conditions of Relevance for Geological Disposal (GLAMOR).SCK.CEN, CEA, Subatech, PNNL, and SRNL EUR 23097. 164p.

Verney-Carron A., Gin S. and Libourel G. (2007) Use of natural and archaeological analogs to validate long-term behaviour of HLW glass in geological disposal conditions. In *Water–Rock-Interaction* (eds. T.D. Bullen and Y. Wang). Balkema, Rotterdam. pp. 659–662.

Zhang L. and Lüttge A. (2008) Aluminosilicate dissolution kinetics: a general stochastic model. *J. Phys. Chem. B* **112**, 1736–1742.

Zhang L. and Lüttge A. (2009) Theoretical approach to evaluating plagioclase dissolution mechanisms. *Geochim. Cosmochim. Acta* **73**, 2832–2849.

Associate editor: Jacques Schott